The accuracy of Generic mesh conformation; the future of facial morphological analysis

Almukhtar, A. A.; Khambay, Balvinder; Ju, C. X.; McDonald, D. J.; Ayoub, E. A.

DOI:
10.1016/j.jpra.2017.08.003

Accepted Manuscript

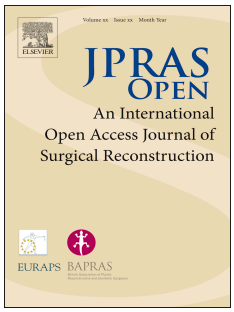

The accuracy of Generic mesh conformation; the future of facial morphological analysis

A.A. Almukhtar, PhD Research Student, B.B. Khambay, Professor of Orthodontics, C.X. Ju, Senior Software Engineer, Honorary Research Fellow, D.J. McDonald, Honorary Professor of Orthodontics, E.A. Ayoub, Professor of Oral & Maxillofacial Surgery

PII: S2352-5878(17)30050-5

DOI: 10.1016/j.jpra.2017.08.003

Reference: JPRA 134

To appear in: *JPRAS Open*

Received Date: 17 November 2016

Revised Date: 2 August 2017

Accepted Date: 5 August 2017

Please cite this article as: Almukhtar AA, Khambay BB, Ju CX, McDonald DJ, Ayoub EA, The accuracy of Generic mesh conformation; the future of facial morphological analysis, *JPRAS Open* (2017), doi: 10.1016/j.jpra.2017.08.003.

The accuracy of Generic mesh conformation; the future of facial morphological analysis

A. A. Almukhtar,
PhD Research Student
Biotechnology and Craniofacial Sciences (BACS) Research Group, Glasgow Dental School, University of Glasgow, Glasgow, UK

B. B. Khambay
Professor of Orthodontics
Dental school, Leeds University.

C. X. Ju
Senior Software Engineer
Medical Device Unit, Department of Clinical Physics and Bioengineering, NHS Greater Glasgow and Clyde, Glasgow, UK
Honorary Research Fellow, Glasgow Dental School, University of Glasgow, Glasgow, UK

D. J. McDonald
Honorary Professor of Orthodontics
Glasgow Dental School, University of Glasgow, Glasgow, UK

E. A. Ayoub
Professor of Oral & Maxillofacial Surgery
MVLS College, Medical school.
University of Glasgow, Glasgow, UK

Corresponding author:
Prof. Ashraf Ayoub
Professor of Oral & Maxillofacial Surgery
Glasgow University
378 Sauchiehall Street, G2 3JZ
Email: ashraf.ayoub@glasgow.ac.uk
Tel 0044 141 2119600

Abstract

3D analysis of the face is required for the assessment of changes following surgery, to monitor the progress of pathological conditions and for the evaluation of facial growth. Sophisticated methods have been applied for the evaluation of facial morphology, the most common one is the dense surface correspondence. The method depends on the application of a mathematical facial mask known as the generic facial mesh for the evaluation of the characteristics of facial morphology. This study was carried out to evaluate the accuracy of the conformation of generic mesh to the underlying facial morphology. The study was conducted on 10 non-patient volunteers. Thirty-four 2mm diameter self-adhesive non-reflective markers were placed on each face. These were readily identifiable on the captured 3D facial image which was captured using Di3D stereophotogrammetry. The markers helped in minimizing the digitization errors during the conformation process. For each case the face was captured 6 times, at rest and at the maximum movements of 4 facial expressions. 3D facial image of each facial expression was analysed. Euclidean distances between the 19 corresponding landmarks on the conformed mesh and on the original 3D facial model provided a measure of the accuracy of the conformation process. For all facial expressions and all corresponding landmarks these distances were between 0.7 and 1.7 mm. The absolute mean distances ranged from 0.73mm to 1.74mm. The mean absolute error of the conformation process was 1.13mm±0.26mm.The conformation of the generic facial mesh proved to be accurate enough for the analysis of the captured 3D facial images.

Introduction

At present the analysis of three-dimensional (3D) facial images has generally been limited to the linear and angular measurements between anatomical landmarks. The operator usually identifies and digitises a set of landmarks resulting in a 3D landmark configuration which is then used for analysis. The limited number of accurately identifiable landmarks does not allow comprehensive analysis of facial morphology.

To overcome this problem the concept of a "generic mesh" has been introduced.[1] The use of generic meshes for analysing biological geometry has previously been reported [2,3]. A generic mesh can be thought of as a "simplified symmetrised facial mask" that contains a known number and distribution of points or "vertices". The triangles or "faces" formed by these vertices are indexed or ordered within the file structure. The generic mesh can be used to standardise the number and distribution of vertices for images of the same individual and between individuals. Using the process of "conformation" the generic facial mesh can be "wrapped" around any facial image based on several anchoring landmarks whist the remaining points are mathematically fitted or elastically deformed to maintain the surface topography of the original 3D image.

The conformation process on the preoperative and postoperative 3D facial images produces two meshes which have the same number of vertices and triangles.Each vertex represents a corresponding point on the preoperative and postoperative conformed meshes. The accuracy of the conformation process of the genric facial meshes will determine the precision in relating the corresdponding facial points for the analysis. A recent study assessing the accuracy of conformation of a generic mesh for the analysis of facial soft tissue changes reported that the method was valid but the accuracy of the conformation was higher toward the middle of the face than the peripheral regions [4]. The study was limited to six anatomical facial regions; left cheek, right cheek, left upper lip, philtrum, right upper lip and chin regions and did not investigate the accuracy of the conformation of the facial mesh at peripheral regions including. forehead, eyes and gonial angle region. This is essential when using generic meshes to analyse pan facial changes especially at peripheral regions i.e. assessing the changes of mandibular gonial region following orthognathic surgery or global facial growth.

Aims

This pilot study was carried out to evaluate the pan-facial accuracy of conformation of a generic mesh.

Materials and methods

Approval has been obtained from the Research ethics committee, MVLS, University of Glasgow Ref: 200150025. Six males and four female healthy adult volunteers with no history of facial deformity or previous surgery in the facial region were recruited and consented to take part in the study.

Participant preparation

Prior to 3D image capture participants were instructed to wear a head cap and then thirty-four 2mm diameter self-adhesive non-reflective black markers (Diamonte, Apparel accessories Ltd, Guangdong, China) were positioned on each subjects' face using an application tool (Pick-it-up vacuum tool, Bead smith, China). The markers (Figure 2 and Table1) were placed around the eyes, nose, mouth and the cheeks in addition to the peripheries of the face including the tragus, gonial angle and the chin areas. These were readily identifiable on the captured 3D facial model which minimized digitization errors of anatomical landmarks during the initial conformation of the facial surface mesh. Fifteen of the markers were used for the conformation process whilst the remaining 19 were used exclusively for the analysis of the accuracy of the method.

For each participant five facial expressions and the baseline relaxed posture were captured using Di3D image capture system (Di3D, Dimensional Imaging, Hillington Park, Glasgow, UK) . The participants were instructed to slide the mandible forward to resemble a prognathic mandible, slide the mandible to the left to resemble mandibular asymmetry, puff the cheek, purse the lip, and smile to test the accuracy of the conformation process of the genric facial mesh with the various facial expressions (Figure 1).

3D image capture and processing

Each participant was positioned for 3D image capture according to a standardised protocol. A Di3D passive stereophotogrammetry system was used to capture each of the six facial

expressions. In total 60 3D images were captured. The images were individually built to produce a 3D facial model which was viewed using Di3D View software (Di3D View, Dimensional Imaging, Hillington Park, Glasgow, UK) and saved in Wavefront (OBJ) format All the captured images were converted from Wavefront (OBJ) to VRML (WRL) files using 3DSMax© software (3DSMax Autodesk, Inc., 2002 Microsoft Corporation). The texture information, dimensional units and the orientation of the image were maintained during the conversion process.

Conformation process

For each individual, the facial mesh in the rest position was used as the generic mesh. The conformation process (elastic deformation) was then performed to warp the generic mesh (at rest) onto each of the other five facial expression images. The in house developed conformation software provided a dual display panel, one for the generic mesh image (at rest image) and the second for one of the five facial expressions. The conformation process was carried out in two steps; *initial semiautomatic non-linear warping* followed by a *final fully automated conformation*. To start the process, fifteen landmarks (Figure 2) were digitized on both the generic mesh as well as on their corresponding locations on the 3D images of each of the five facial expressions. Each landmark was digitized at the centre of the 2mm prefixed markers on the face, Figure 2. Based on the 15 selected corresponding landmarks, the generic mesh of 3D facial image at rest was warped to each of the facial images (the target image) of the five expressions. To achieve the final conformation process the generic mesh was elastically deformed (warped) over the target image to resemble the shape of the mesh of the facial expression. The conformed images, of the five facial expressions, were exported as a VRML (WRL) file and saved for further analyses. The procedure was repeated for the ten participants and produced 50 conformed meshes in total.

Errors of the method

To assess the errors of the method, ten randomly selected images, one from each case, were landmarked twice, with two weeks interval by the same operator (AAM). Both the absolute directional (x, y, and z) distances and the Euclidean distances between the repeated digitisation of the same landmark were calculated.

Analysis

Following conformation of generic mesh at the rest position and to each of the facial expressions, the 19 landmarks which not used during conformation were used for the analysis of the accuracy of the process. ,. The mean Euclidian distance between the actual postion of these landmarks on the non-conformed expression mesh and the same landmarks on the conformed generic mesh, indicated the accuracy of the conformation process. These were for each facial expression of the 10 volunteers, The closer the mean distance to zero, the more accurate the conformation process is.

In addition, the classical *inter-surface distance* (mean absolute distances) were measured between the non-conformed surface mesh and the conformed generic mesh based on the 90^{th} percentile of the vertices of these meshes. A distance colour map was generated for visual illustration of the conformation process. The data produced from each set of measurements were saved in Microsoft Excel (Microsoft®, Redmond, CA) file for further analysis.

Results

Error of the method

For errors of the landmarking the mean Euclidean distance and standard deviation for each of the 34 landmarks are shown in Table 2. The overall mean error for all the landmarks was 0.25±0.10mm. Landmarks 6 (Nasion) and 8 (Endocanthion left) had the lowest error 0.11±0.05mm and 0.11±0.10mm respectively whilst landmark 30 (Gonion left) had the largest error 0.53±0.62mm.

Accuracy of conformation

Euclidian distances between the 19 landmarks on the non-conformed expression mesh and the same landmarks on the conformed generic meshprovided a measure of the accuracy of the conformation process (Table 3). The minimum mean Euclidean distance between the corresponding landmarks was at Philtrum crest right, 0.73±0.24mm (95% CI 0.62mm to 0.99mm) whilst the maximum distance was at Gonion right, 1.74±0.64mm (95% CI 1.33mm to 2.37mm). The mean Euclidean distance error of the conformation process was 1.13±0.26mm.

The effect of each facial expression on the accuracy of the conformation is shown in Table 4, based on the accuracy of the conformation process the five facial expressions were ranked in ascending order starting with the lateral mandible shift, lip purse, forward mandible shift, cheek puff and smile. The lowest errors (1.06±0.33mm) of the conformation process of the facial mesh were associated with the lateral mandible shift expression, the maximum inaccuracy of the conformation process was related to maximum smile, this was 1.46±0.51mm.

Table 3 shows the accuracy of the conformation process based on the mean absolute distances between the conformed and the original meshes. The largest distance was 0.06mm which was observed in subject 3 across all facial expressions.

Discussion

Dense correspondence analysis has been reported as an efficient method of analysing morphological changes which may explain its broad applications in the medical field [(3)]. However, despite its accuracy and comprehensiveness in soft tissue analyses, this approach is largely dependent on “3D model elastic deformation” in which the generic facial mesh is elastically deformed to reproduce the individual’s facial features. The initial step of the conformation process involved the translation of the corresponding landmarks to match their positions of the target image followed by the elastic deformation to minimize bending energy (thin plate spline). This process included both shape and positional change. In this study the six facial postures were captured at the same session which provided a relatively

close starting point for the conformation process. Despite the fact that only 10 volunteers participated in this study, each of the facial postures was considered an individual case, therefore; the total number of the images involved in the study was 50. A total of 15 landmarks were used to execute the conformation procedure. To eliminate bias, these landmarks were excluded from the analysis of the accuracy of the conformation procedure.

The accuracy of the conformation process has previously been reported[5,6]. In these studies, the accuracy was determined by measuring the inter-surface distance between the conformed mesh and the target models. The disadvantage of this approach is that the magnitude of error is measured as the distance between the closest points on the two surface meshes, namely the target model and the conformed mesh, not the distances between the actual anatomical corresponding points. Measuring the closest distance between two meshes would not necessarily detect the potential sliding of the surface meshes over one another during the conformation process which would provide a misleading low estimate of the conformation errors. On the other hand, the assessment of the accuracy of the conformation process based on specific landmarks also carries the risk of overestimating the accuracy of the conformation process since only a single point on the mesh is analysed whilst the remainder of the mesh is not assessed.

The Euclidian distance between the actual landmarks on the non-conformed mesh and the landmarks on the conformed generic mesh, for the same facial expression, was used as a measure of accuracy of the conformation process. Although this was not a comprehensive surface based analysis, its robustness was maximised by carefully selecting the landmarks to represent various anatomical regions of the face which was thought to be clinically relevant.

The analysis was repeated using the classical inter-surface distances based on the 90^{th} percentile of the vertices of the two meshes and measuring the mean distances between the conformed mesh and original mesh for all facial expressions. This measure takes into account the direction of error and produces positive and negative values, which depend on the spatial location of the meshes relative to each other. Despite the fact that these measurements are descriptive to the magnitude and the direction of the conformation errors, the mean value of these measurements are underestimated as positive and the

negative measurements and would cancel each other. On the other hand the Euclidean distances measures the shortest distances between corresponding points of the two surface meshes irrespective of the directionality of the mismatch between the two surface meshes, therefore, the arithmetic average value of these distances is more meaningful. As expected the error based on the mean absolute distances is much smaller than those based on the Euclidian distances.

Two main factors may contribute to the errors in the conformation process; first and most important is the accuracy and reproducibility of the digitization of the landmarks which are used in the initial conformation stage. This was minimised in the present study using pre-landmarking. The second source of errors depnds on the is a of deficiency in the algorithm of the conformation process [(5)].

To reduce the effect of landmarking errors, which impacts on the reliability of the conformation process, round 2mm markers were pre-placed on 34 anatomical points on each participant face. The use of pre-landmark placement significantly reduced the landmarking error and allowed the conformation process to be analysed comprehensively by eliminating this potential source of error [(7)]. The rounded shape of the landmark facilitated accurate landmarks digitization, with a mean error of 0.23mm±0.11mm.

The presented innovative approach provides a useful tool for 3D analysis of the face; it provides comprehensive evaluation of the morphological characteristics which is more superior than the assessment at a limited set of individual landmarks. The method allows the analysis of facial asymmetries and both the typical and abnormal growth pattern. It can be applied for the evaluation of a sequence of 3D facial images (4D) for the analysis of the dynamics of facial expressions. We expect the method to be fully integrated as a clinical tool with various surgical specialities to improve the quality of diagnosis and prediction planning of corrective facial surgeries. The limitation associated with the visualisation of 3D facial model on a flat screen can be solved with the production of 3D objects using the innovation of 3D printing and rapid prototyping.[(8)]

The results of this study confirmed that landmarks around the lips and nose (in the mid-line) were associated with lower level of conformation errors compared to those around the borders of the image such as cheeks, gonial angle regions which is in agreement with previous studies [4]. This might be due to the lack of details of surface topography upon which the elastic deformation relied in conjunction with absence of well-defined landmarks around the lower border and gonial angle region. This should be taken onto account when using this technique in facial analysis following orthognathic surgery. The changes around the lower border and gonial angle should be viewed with caution as they showed a higher level of inaccuracy as indicated by the upper 95% confidence limit of around 2.0mm

Conclusions

The conformation procedure has a 1-2mm level of accuracy, with a higher level of accuracy in the midline and less peripherally. This technique has broad clinical applications including facial analysis of the impact of orthognathic surgery in changing facial morphology and monitoring of facial growth.

Legends of the figures

Figure 1 The six facial movements that were recorded for the study

Figure 2 The anatomical position of facial landmarks

Figure 3 The fifteen landmarks used for the initial conformation phase.

Funding and conflict of Interest:None

References

1. Khambay B, Ullah R. Current methods of assessing the accuracy of three-dimensional soft tissue facial predictions: technical and clinical considerations. Int J Oral Maxillofac Surg 2015;44(1):132–8.

2. Claes P, Walters M, Clement J. Improved facial outcome assessment using a 3D anthropometric mask. Int J Oral Maxillofac Surg 2012;41(3):324–30.

3. Claes P, Walters M, Vandermeulen D, Clement JG. Spatially-dense 3D facial asymmetry assessment in both typical and disordered growth. J Anat 2011;219(4):444–55.

4. Cheung MY, Almukhtar A, Keeling A, Hsung T-C, Ju X, McDonald J, et al. The Accuracy of conformation of a generic surface mesh for the analysis of facial soft tissue changes. PLoS One 2016;11(4):e0152381.

5. Zhili Mao, Xiangyang Ju, J. Paul Siebert, W. Paul Cockshott AA. Constructing dense correspondences for the analysis of 3D facial morphology. Pat Recog Lett 2006;27:597–608.

6. Chabanas M, Luboz V, Payan Y. Patient specific finite element model of the face soft tissues for computer-assisted maxillofacial surgery. Med Image Anal 2003;7:131–51.

7. Aynechi N, Larson BE, Leon-Salazar V, Beiraghi S. Accuracy and precision of a 3D anthropometric facial analysis with and without landmark labeling before image acquisition. Angle Orthod 2011;81(2):245–52.

8. Rengier F, Mehndiratta A, von Tengg-Kobligk H, Zechmann CM, Unterhinninghofen R, Kauczor HU, Giesel FL. 3D printing based on imaging data: review of medical applications. Int J CARS 2010;5:335-41

Table 1 Landmarks definitions

	Abbr.	Landmarks	Definition
1	Eb(R)	Eyebrows-R	The point just above the eyebrows at a vertical line from the pupil.
2	Gla	Glabella	Most prominent midline point between eyebrows
3	Eb(L)	Eyebrows-L	The point just above the eyebrows at a vertical line from the pupil.
4	Ex(R)	Exocanthion-R	Outer commissure of the eye fissure
5	En(R)	Endocanthion-R	Inner commissure of the eye fissure
6	Na	Nasion	Deepest concavity in the midline at the root of the nose
7	Ex(L)	Exocanthion-L	Outer commissure of the eye fissure
8	En(L)	Endocanthion-L	Inner commissure of the eye fissure
9	Sbtr(R)	Subtragion-R	The most anterior inferior point of the anterior inferior attachment of the ear helix, just above the ear lob
10	Sbtr(R)1/3*	Subtragion-R (1/3)	One third the distance from Sbtr(R) to Ala(R)
11	Sbtr(R)2/3*	Subtragion-R (2/3)	Two third the distance from Sbtr(R) to Ala(R)
12	Ala(R)	Alar curvature-R	Most lateral point on alar contour
13	Ab(R)	Alar base-R	Junction between the right nostril and upper lip
14	Prn	Pronasale	Most protruded point of the apex nasi (tip of the nose)
15	Ab(L)	Alar base-L	Junction between the right nostril and upper lip
16	Ala(L)	Alar curvature-L	Most lateral point on alar contour
17	Sbtr(L)1/3*	Subtragion-L (1/3)	One third the distance from Sbtr(L) to Ala(L)
18	Sbtr(L)2/3*	Subtragion-L (2/3)	One third the distance from Sbtr(L) to Ala(L)
19	Sbtr(L)	Subtragion-L	The most anterior inferior point of the anterior inferior attachment of the ear helix, just above the ear lobe
20	Go(R)	Gonion-R	The most lateral point of the cheeks close to mandibular angle.
21	Go(R)1/3*	Gonion-R 1/3	One third the distance from Go(R) to Ch(R)
22	Go(R)2/3*	Gonion-R 2/3	The third the distance from Go(R) to Ch(R)
23	Ch(R)	Cheilion-L	Point located at lateral labial commissure
24	PhL(R)	Philtrum crest-R	The tip of the right philtral ridge at the upper lip vermilion border
25	Ls	Labial superius	Midpoint of the upper vermilion line
26	PhL(L)	Philtrum crest-L	The tip of the right philtral ridge at the upper lip vermilion border
27	Ch(L)	Cheilion-L	Point located at lateral labial commissure
28	Go(L)2/3*	Gonion-L 1/3	One third the distance from Go(L) to Ch(L)
29	Go(L)1/3*	Gonion-L 2/3	The third the distance from Go(L) to Ch(L)
30	Go(L)	Gonion-L	The most lateral point of the cheeks close to mandibular angle.
31	Li+3*	Labial inferius	Mid-point on the lower vermilion line 3mm higher than Li
32	Li	Labial inferius	Mid-point of the lower vermilion line
33	Pog+3*	Pogonion+3	Midline point 3mm higher than pogonion
34	Pog	Pogonion	Most prominent midline point of the chin

Table 2 Mean Euclidean distance and standard deviation for landmarking errors for each of the 34 landmarks.

Landmark number	Abbreviation	Landmarks	Mean (mm)	SD (mm)	95% Confidence Interval	
					Lower	Upper
1	Eb(R)	Eyebrows-Right	0.20	0.15	0.08	0.3
2	Gla	Glabella	0.17	0.10	0.09	0.24
3	Eb(L)	Eyebrows-Left	0.15	0.05	0.11	0.19
4	Ex(R)	Exocanthion-Right	0.14	0.10	0.06	0.21
5	En(R)	Endocanthion-Right	0.13	0.10	0.05	0.2
6	Na	Nasion	0.11	0.05	0.05	0.14
7	Ex(L)	Exocanthion-Left	0.18	0.12	0.09	0.27
8	En(L)	Endocanthion-Left	0.11	0.10	0.03	0.18
9	Sbtr(R)	Subtragion-Right	0.18	0.12	0.07	0.24
10	Sbtr(R)1/3*	Subtragion-Right (1/3)	0.16	0.09	0.09	0.23
11	Sbtr(R)2/3*	Subtragion-Right (2/3)	0.22	0.12	0.13	0.30
12	Ala(R)	Alar curvature-Right	0.21	0.17	0.06	0.32
13	Ab(R)	Alar base-Right	0.22	0.16	0.13	0.22
14	Prn	Pronasale	0.18	0.09	0.12	0.24
15	Ab(L)	Alar base-Left	0.22	0.09	0.13	0.27
16	Ala(L)	Alar curvature-Left	0.19	0.12	0.08	0.27
17	Sbtr(L)1/3*	Subtragion-Left (1/3)	0.16	0.11	0.07	0.24
18	Sbtr(L)2/3*	Subtragion-L eft (2/3)	0.30	0.27	0.09	0.49
19	Sbtr(L)	Subtragion-Left	0.34	0.23	0.13	0.47
20	Go(R)	Gonion-Right	0.17	0.07	0.09	0.21
21	Go(R)1/3*	Gonion-Right 1/3	0.16	0.08	0.10	0.20
22	Go(R)2/3*	Gonion-Right 2/3	0.21	0.11	0.13	0.29
23	Ch(R)	Cheilion-Left	0.15	0.08	0.09	0.21
24	PhL(R)	Philtrum crest-Right	0.22	0.11	0.12	0.30
25	Ls	Labial superius	0.31	0.28	0.11	0.50
26	PhL(L)	Philtrum crest-Left	0.16	0.10	0.08	0.24
27	Ch(L)	Cheilion-Left	0.19	0.09	0.12	0.25
28	Go(L)2/3*	Gonion-Left 1/3	0.25	0.17	0.11	0.37
29	Go(L)1/3*	Gonion-Left 2/3	0.27	0.07	0.17	0.31
30	Go(L)	Gonion-Left	0.53	0.62	0.07	0.97
31	Li+3*	Labial inferius	0.36	0.20	0.21	0.50
32	Li	Labial inferius	0.43	0.36	0.15	0.68
33	Pog+3*	Pogonion+3	0.43	0.29	0.21	0.63
34	Pog	Pogonion	0.33	0.10	0.23	0.4
Overall Mean			**0.25**	**0.10**		

*** Constructed landmarks**

Table 3 Mean absolute distance between meshes (mm).

	Lateral mandible shift		Cheek puff		Forward mandible shift		Smile		Lip purse	
Cases	Absolute Mean	SD	Absolute Mean	SD	Absolute Mean	SD	Absolute Mean	SD	Absolute Mean	SD
1	0.04	0.08	0.04	0.07	0.04	0.06	0.04	0.07	0.04	0.09
2	0.00	0.03	0.00	0.07	0.00	0.02	0.00	0.02	0.00	0.03
3	0.05	0.1	0.06	0.1	0.06	0.1	0.06	0.1	0.06	0.11
4	0.00	0.03	0.00	0.01	0.00	0.01	0.00	0.01	0.00	0.02
5	0.02	0.03	0.02	0.01	0.02	0.03	0.02	0.06	0.02	0.04
6	0.02	0.02	0.02	0.01	0.02	0.01	0.02	0.01	0.02	0.01
7	0.02	0.04	0.02	0.03	0.02	0.03	0.02	0.03	0.02	0.03
8	0.00	0.01	0.00	0.02	0.00	0.01	0.00	0.01	0.00	0.03
9	0.02	0.17	0.02	0.12	0.00	0.05	0.00	0.02	0.00	0.05
10	0.00	0.02	0.00	0.01	0.00	0.01	0.00	0.01	0.00	0.01

Table 4 shows the mean Euclidean distances (mm) of the 19 corresponding landmarks between the conformed and original mesh for all facial expressions.

Landmark Number	Abbreviations	Landmarks names	Mean (mm)	SD (mm)	95% Confidence Interval	
					Lower	Upper
1	Eb(R)	Eyebrows-Right	1.27	0.34		
2	Gla	Glabella	0.77	0.36	1.11	1.65
3	Eb(L)	Eyebrows-Left	1.19	0.31	0.56	1.10
10	Sbtr(R)1/3*	Subtragion-Right (1/3)	1.20	0.45	1.06	1.53
11	Sbtr(R)2/3*	Subtragion-Right (2/3)	1.21	0.39	0.93	1.68
12	Ala(R)	Alar curvature-Right	1.17	0.46	1.02	1.6
16	Ala(L)	Alar curvature-Left	1.07	0.32	0.87	1.55
17	Sbtr(L)1/3*	Subtragion-Left (1/3)	1.18	0.40	0.89	1.38
18	Sbtr(L)2/3*	Subtragion-Left (2/3)	1.14	0.34	0.96	1.59
20	Go(R)	Gonion-Right	1.74	0.64	0.97	1.50
21	Go(R)1/3*	Gonion-Right 1/3	1.37	0.55	1.33	2.37
22	Go(R)2/3*	Gonion-Right 2/3	0.76	0.43	1.10	1.88
24	PhL(R)	Philtrum crest-Right	0.81	0.22	0.49	1.17
26	PhL(L)	Philtrum crest- Left	0.73	0.24	0.72	1.07
28	Go(L)2/3*	Gonion-Left 1/3	1.05	0.64	0.62	0.99
29	Go(L)1/3*	Gonion-Left 2/3	1.41	0.43	0.63	1.56
30	Go(L)	Gonion-Left	1.44	0.40	1.22	1.85
32	Li	Labial inferius	0.96	0.34	1.24	1.83
34	Pog	Pogonion	0.97	0.83	0.77	1.24
Overall mean distance			**1.13**	**0.26**	**0.43**	**1.65**

*** Constructed landmarks**

Table 5 Mean Euclidean distance between the corresponding landmarks for each facial expression (mm)

Landmark number	Landmarks		Lateral mandible shift	Cheek puff	Forward mandible shift	Smile	Lip purse	Mean (mm)	SD (mm)
			Mean	Mean	Mena	Mean	Mean		
1	Eb(R)	Eyebrows-R	1.87	1.1	1.25	1.62	1.07	1.38	0.35
2	Gla	Glabella	1.08	0.58	1.01	0.97	0.50	0.83	0.27
3	Eb(L)	Eyebrows-L	1.23	1.23	1.43	1.50	1.08	1.29	0.17
10	SbtrR 1/3	Subtragion-R (1/3)	1.09	1.65	0.82	1.85	1.11	1.3	0.43
11	Sbtr R2/3	Subtragion-R (2/3)	1.08	1.95	0.78	1.63	1.10	1.31	0.47
12	Ala(R)	Alar curvature-R	0.96	1.76	0.98	1.02	1.35	1.21	0.35
16	Ala(L)	Alar curvature-L	0.99	1.67	0.66	0.93	1.44	1.14	0.41
17	Sbtr L1/3	Subtragion-L (1/3)	0.83	2.03	0.88	1.60	1.04	1.28	0.52
18	Sbtr L2/3	Subtragion-L (2/3)	0.94	1.62	0.80	1.81	1.01	1.24	0.45
20	Go(R)	Gonion-R	1.40	1.58	2.49	2.51	1.27	1.85	0.60
21	Go(R) 1/3	Gonion-R 1/3	1.31	1.76	0.97	1.80	1.62	1.49	0.35
22	Go(R) 2/3	Gonion-R 2/3	0.70	0.84	0.77	0.97	0.87	0.83	0.10
24	PhL(R)	Philtrum crest-R	0.69	1.03	0.72	1.16	0.87	0.89	0.20
26	PhL(L)	Philtrum crest-L	0.53	0.90	0.66	1.11	0.83	0.81	0.23
28	Go(L) 2/3	Gonion-L 1/3	0.78	1.25	1.07	1.30	1.08	1.10	0.20
29	Go(L) 1/3	Gonion-L 2/3	0.99	1.65	1.38	2.11	1.53	1.53	0.41
30	Go(L)	Gonion-L	1.51	1.41	1.35	2.15	1.23	1.53	0.36
32	Li	Labial inferius	1.39	0.68	1.16	0.61	1.19	1.01	0.34
34	Pog	Pogonion	0.74	0.76	1.89	0.99	0.82	1.04	0.48
Overall mean			1.06	1.34	1.11	1.46	1.11	**1.21**	**0.28**
SD			0.33	0.45	0.46	0.51	0.27		

		
Relax (repose)	Cheek blow	Chin lateral shift
		
Lop purse	Chin forward shift	Smile

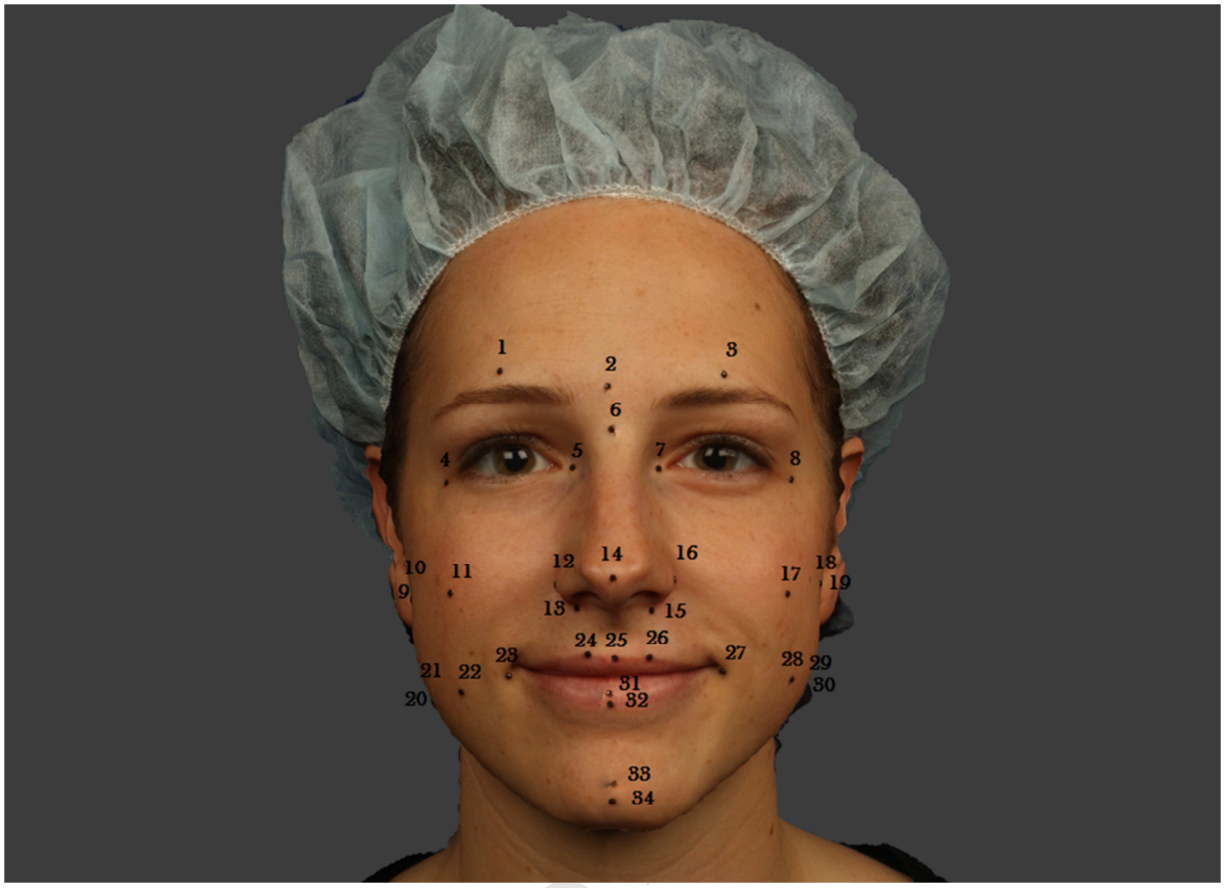
1
2
3
6
4
5
7
8
10
11
12
14
16
17
18
19
9
13
15
24
25
26
23
27
28
29
21
22
31
30
20
32
33
34

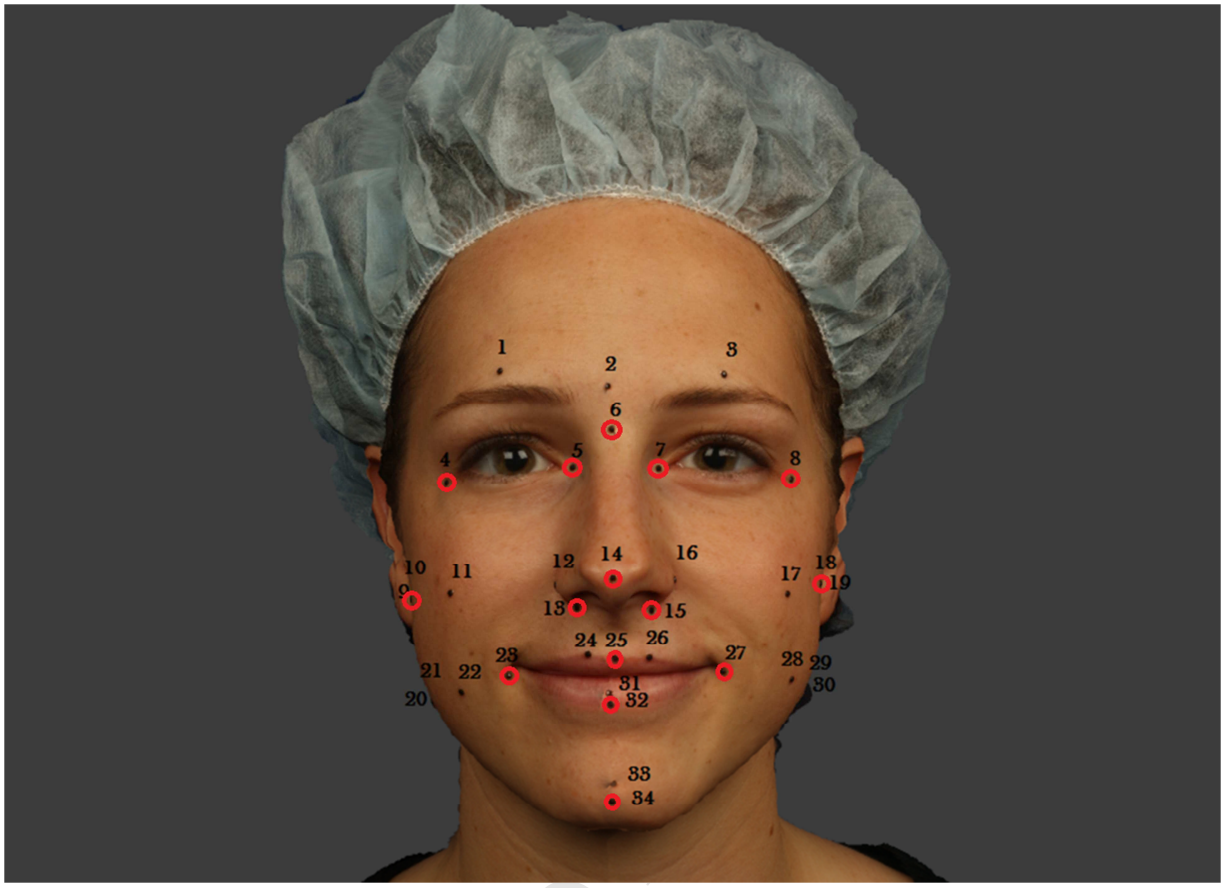
1
2
3
6
4
5
7
8
10
11
12
14
16
17
18
19
9
13
15
24
25
26
28
27
28
29
21
22
31
30
20
32
33
34